Permeation of Polychlorinated Biphenyls Through Lipid Membranes: Classical MD and QM/MM-EDA Analysis

Nicolás Ramos-Berdullas(✉), Álvaro Pérez-Barcia, and Lorena Ruano

Department of Physical Chemistry, University of Vigo, Lagoas-Marcosende s/n, 36310 Vigo, Spain
nicolas.ramos@uvigo.es

Abstract. Persistent organic compounds, particularly those of industrial origin, are highly toxic, bioaccumulative, persistent, and capable of traveling long distances. The World Health Organization even considers some of them potential carcinogens. In the marine environment, polychlorinated biphenyls (PCBs) accumulate in sediments, leading to continuous exposure and potentially causing adverse effects on ecosystems and food chains. In particular, concentrations of seven key PCBs (IUPAC numbers 28, 52, 101, 118, 138, 153 and 180) are usually closely monitored. Despite advances in understanding the metabolic processes of PCBs, their absorption and diffusion mechanisms across cell membranes remain insufficiently understood. These membranes act as reservoirs for PCBs, prolonging chronic exposure. In this study, we investigate the permeation process of these compounds across lipid membranes by means of classical molecular dynamics (CMD) in combination with the umbrella sampling approach, using a model composed of 128 1,2-dioleoyl-sn-glycero-3-phosphocholine lipids (DOPC). The free energy profile shows the penetration process is largely favoured thermodynamically, with a progressively decrease of the energy until reaching the energy minima close to the centre of the membrane. The analysis of key regions along the diffusion pathway is particularly relevant for studying intermolecular interactions between PCBs and lipid bilayers. Therefore, the characterization of contaminant-membrane interactions was initially conducted using a combination of quantum mechanics/molecular mechanics (QM/MM) calculations and energy decomposition analysis (EDA). This approach provides deeper insight into the underlying mechanisms, including the contributions of electrostatic, exchange, repulsion, and polarization interactions, which together elucidate the permeation process.

Keywords: Persistent Organic Pollutants · Polychlorinated Biphenyls · Lipid Membranes · Molecular Dynamics · QM/MM · EDA

1 Introduction

In the present world, pollution represents one of the greatest challenges for the global population. The international community has developed regulations to control and reduce pollutant emissions and existing contamination, with an emphasis on studying the action

© The Author(s), under exclusive license to Springer Nature Switzerland AG 2026
O. Gervasi et al. (Eds.): ICCSA 2025 Workshops, LNCS 15897, pp. 28–38, 2026.
https://doi.org/10.1007/978-3-031-97660-5_3

mechanisms to detect and eliminate chemical agents, such as persistent organic pollutants (POPs) [1]. These compounds, mainly of industrial origin, are characterized by their high toxicity, resistance to natural degradation, high bioaccumulation, and significant ability to travel long distances [2], posing an environmental and health risk, according to the Stockholm Convention and the WHO [3].

In the marine environment, persistent pollutants can enter through the atmosphere or from urban and industrial inputs [4, 5], associating with organic particles and accumulating on the seabed for years. This process exposes living organisms to these compounds through ingestion, leading to their introduction into the food chain, or through the resuspension of sediments, causing negative effects on ecosystems and, by extension, on health. Among persistent organic pollutants, polychlorinated biphenyls (PCBs) stand out due to their significant presence in this environment. These substances, lipophilic in nature, preferentially accumulate in the fatty tissues of living organisms [6, 7]. They form a group of 209 congeners with various ecotoxicological properties, which vary depending on the degree of chlorination and the position of chlorine atoms in the molecule. Additionally, several studies conducted along the western coast of Europe reveal that marine sediments in this area exceed the maximum acceptable ecotoxicological values [8, 9], identifying it as a significant source of PCB contamination. It is important to note that, in marine pollution monitoring and control programs, only seven of the most representative congeners are included: six non–dioxin-like (NDL-PCB) (IUPAC no. 28, 52, 101, 138, 153, and 180), and one dioxin-like (DL-PCB) (IUPAC no. 118) (see Fig. 1). The sum of the concentrations of these compounds is referred to as SCB7 and is used as the main indicator of PCB contamination.

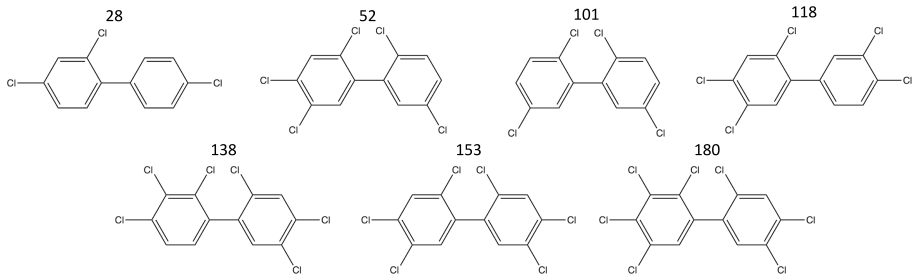

Fig. 1. Schematic representation of the PCBs that make up the SCB7 set.

Despite advances in the study of PCB metabolism, the absorption and diffusion process of these compounds across cell membranes remains insufficiently understood. Understanding this mechanism is critical for elucidating the toxicokinetics of PCBs and assessing the risks associated with their exposure. Cell membranes, in addition to acting as a barrier, function as reservoirs for PCB storage, becoming an internal source of chronic exposure to these contaminants [6]. In this context, computational simulations using classical methods provide valuable information on the thermodynamics and kinetics of dehydration and diffusion processes of PCBs across membranes. Quantum mechanical models, on the other hand, represent a promising tool for analyzing molecular

interactions between pollutants and cell membranes, facilitating a more precise description of the structural and functional changes these compounds induce in the biological environment.

Herein, a comparative study of the permeation of the aforementioned PCBs molecules through a lipid membrane model has been conducted using umbrella sampling combined with classical molecular dynamics (CMD) in order to evaluate the role that membrane permeability plays in the relative toxicity of these compounds. The aim of our work has been extended to shed more light on the origin and nature of the intermolecular interactions governing the process, particularly at the free energy minima, where the molecular environment changes due to the hydrophilic and hydrophobic regions of the lipid bilayer. To this end, a hybrid QM/MM energy decomposition analysis (QM/MM-EDA) has been initially applied at the free energy minima along the permeation path of PCBs through biological membranes (both DL-PCB and NDL-PCB). This approach has been successfully applied to other persistent organic pollutants such as chlorinated dibenzo-p-dioxins and dibenzofurans, but this is the first time that the permeation of PCBs through biological membranes has been studied at the quantum mechanical level. Finally, the results presented here also serve to assess the capability of classical force fields to represent the intermolecular interactions of these molecules with the lipid bilayer and evaluate strategies to accurately simulate the interactions involved in biological systems.

2 Methodology

2.1 CMD Simulations

The dynamic simulations of the absorption and distribution process of the compounds that make up SCB7 was carried out using a lipid membrane composed of 1,2-dioleoyl-sn-glycero-3-phosphatidylcholine (DOPC) units. The bilayer contained 128 DOPC lipids, evenly distributed between the upper and lower layers. The membrane was placed in a rectangular box with periodic boundary conditions applied in all three spatial dimensions. Additionally, to mimic physiological conditions, the membrane was solvated by including a water layer of 22.5 Å on each side (approximately 37 water molecules per lipid) and a 0.15 M concentration of KCl ions. The Lipid17 force field [10] was used to describe the lipid bilayer, while the TIP3P model was used to describe the water molecules. The K^+ and Cl^- ions were represented using appropriate Amber parameters.

The resulting structure underwent a relaxation process to ensure system stability before further analysis. Initially, a 10,000-step minimization was performed, transitioning from a steepest descent to a conjugate gradient minimization midway through the simulation. This was followed by a sequential heating phase: a 5 ps run increased the temperature to 100 K in the constant temperature and volume ensemble (NVT), followed by a 100 ps run that heated the system to 303 K in the constant temperature and pressure ensemble (NPT). Positional restraints were applied to the lipid molecules throughout the heating process.

Next, ten sequential runs of 500 ps were performed to ensure the equilibration of the periodic boundary conditions of the system, followed by a production step that lasted 125 ns. These simulations were conducted in the NPT ensemble under the same

conditions as the second heating step. Finally, a randomly selected snapshot was extracted from the production step to represent the final configuration of the system.

Each PCB was inserted at 32 Å from the center of mass of the relaxed DOPC membrane, with the intramolecular and Lennard-Jones parameters of the compounds provided by the General Amber Force Field (GAFF) [11]. To calculate the atomic charges, the geometries of the previously obtained conformational minima were optimized using the M06-2X functional and the 6-311G(d,p) basis set, followed by the application of the Merz-Singh-Kollman scheme at the same level of theory.

Next, a minimization of 20,000 steps was performed, again using the conjugate gradient method in the second half. The system was then heated to 303 K, imposing certain positional restraints of 10 kcal/mol·Å^2 and 5 kcal/mol·Å^2 on the lipid bilayer and the PCB, respectively. The heating was carried out in the NVT ensemble for 1 ns. Subsequently, four 5 ns runs were performed in the NPT ensemble to equilibrate the system before the accelerated simulation. Each run maintained the pressure and temperature at the desired values of 1 bar and 303 K, respectively, while gradually reducing the initial positional restraints mentioned earlier on the lipid bilayer and the PCB. Molecular dynamics simulations were executed using the pmemd CUDA implementation of the Amber program [12].

Once the system was equilibrated, the permeation processes of two conformers with different degrees of chlorination were simulated using umbrella sampling, except for PCB no. 28, which, due to its symmetry, has only one conformer. The reaction coordinate was defined as the distance along the z-axis (perpendicular to the lipid bilayer) between the contaminant's center of mass and the membrane, with 0 Å representing the contaminant at the center of the membrane. The initial reaction coordinate was set at 32.0 Å from the membrane center and was divided into 32 windows, each spanning 1.0 Å. As a result, the full simulation of contaminant penetration from the aqueous phase to the membrane center lasted 640 ns, with each window simulated for 20 ns. Finally, the Weighted Histogram Analysis Method (WHAM) was applied to obtain the free energy profiles [13].

2.2 QM/MM EDA Calculations

The interaction energy, E_{int}, between two molecular systems A and B is defined as:

$$E_{int} = E_{AB} - \left(E_A^{AB} - E_B^{AB}\right) \tag{1}$$

where E_{AB}, represents the energy of the complex, and $E_A^{AB}$and E_B^{AB} correspond to the energies of the isolated systems, calculated in the same geometry and using the same basis set as in the complex.

The EDA scheme used in this study to analyze non-covalent interactions partitions the complex energy, expressed in terms of the one-electron density, density matrix, and exchange-correlation density (see Eq. 2), into perturbed and unperturbed components [14]. Additionally, a second-order perturbation approach is applied to further decompose the polarization energy [15]. Consequently, the total interaction energy from Eq. (1) is divided into electrostatic (E_{elec}), Pauli repulsion (E_{Pau}), induction (E_{ind}), and dispersion

(E_{disp}) contributions.

$$E_{int} = E_{elec} + E_{Pau} + E_{ind} + E_{disp} \tag{2}$$

When a QM/MM electrostatic embedding is introduced in the calculations, the electrostatic potential, $\hat{V}_{MM}(r)$, associated to the MM charges, q_i,

$$\hat{V}_{MM}(r) = \sum_{i=1}^{NA_{MM}} \frac{q_i}{|r - R_i|} \tag{3}$$

must be added to both or one of the nuclei potential operators, $\hat{v}_{N_A}(r)$ and $\hat{v}_{N_B}(r)$, as well as to the nuclear repulsion energy in order to get the energy decomposition of Eq. (2) at QM/MM level of theory.

This scheme, used in the study of membrane-pollutant interactions, requires the system to be divided into two subsystems as the pollutant molecule (A) and the DOPC membrane together with water molecules and ions (B). Additionally, this analysis also requires a description of the interaction region using a QM theory level, combined with a classical approach as the electrostatic embedding to represent the environmental effects. The optimal QM region should include the pollutant and the minimum number of DOPC molecules necessary to ensure the convergence of the total pollutant-lipid interaction energy and its components. Thus, subsystem A is fully described at the QM level, whereas the complex and subsystem B are described at QM/MM level. In our particular case, $\hat{V}_{MM}(r)$, has been added to $\hat{v}_{N_B}(r)$ and to the nuclear term of the electrostatic energy as follows [16, 17],

$$\hat{v}_{N_B}^{MM}(r) = \hat{v}_{N_B}(r) + \hat{V}_{MM}(r) \tag{4}$$

QM/MM calculations were performed using the Gaussian16 software package [18], employing density functional theory (DFT) with the M06-2X functional and 6-31G(d,p) basis set—well-suited for non-covalent interactions without empirical dispersion corrections [19]. The QM/MM-EDA scheme required three electronic structure calculations: one for the full complex (pollutant plus solvated membrane), one for the solvated membrane, and one for the pollutant alone. Gaussian input files were automatically generated using MoBioTools [20, 21], ensuring the complete basis set was applied to prevent basis set superposition errors. Electrostatic embedding was applied, incorporating atomic charges from the MM region, which were extracted from Amber CMD simulations and included in Gaussian input files via MoBioTools. The interaction energy and its components were computed using the EDA-NCI program [22].

3 Results and Discussion

3.1 Optimization Geometrical and Energy Stabilization

The geometric optimization and vibrational analysis of the PCB set were performed using the Gaussian16 software [18]. The optimized geometries and ground-state energies were obtained at the density functional theory (DFT) level, employing the M06-2X functional [19] in combination with the 6-311G(d,p) basis set.

The rotation between the phenyl groups of different PCBs was analyzed due to its importance in estimating and examining free energy profiles during the entry and diffusion of these compounds. The inclusion of an additional reaction coordinate, beyond that associated with membrane penetration, increases the complexity of the study, as it necessitates analyzing a free energy surface rather than a one-dimensional profile. To address this issue, DFT calculations were performed by varying the angle between the phenyl rings, thereby obtaining the potential energy profiles associated with the torsional coordinate (see Fig. 2).

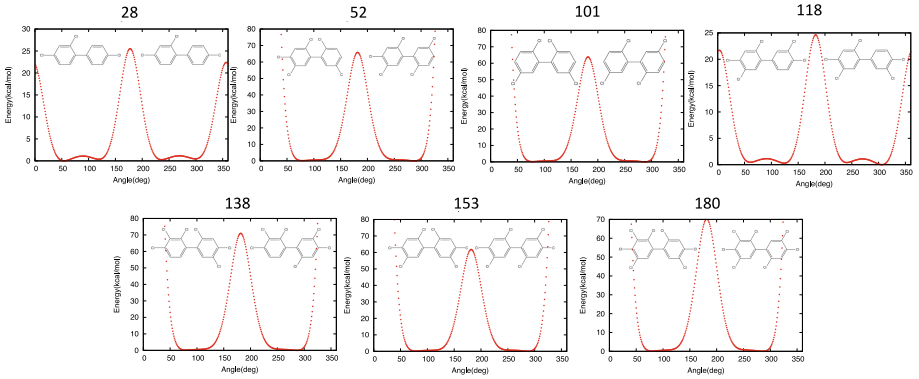

Fig. 2. Potential energy profiles of different PCBs, including schematic representations of the resulting structures with dihedral angles less than 180° and greater than 180°.

The calculation results revealed that PCBs with substituents in the ortho position exhibit a significantly higher energy barrier compared to those lacking chlorination in these positions. Nevertheless, in all cases, symmetric profiles with substantial energy barriers around 180° were observed, as reported in Table 1.

Table 1. Energy barriers (kcal/mol) for the relative maxima around 180°.

IUPAC no.	Angle	Energy	IUPAC no.	Angle	Energy
28	177	25.52	138	182	70.95
52	181	65.82	153	181	61.79
101	182	63.81	180	182	70.21
118	183	24.62			

Furthermore, the energy values and configurations obtained through quantum calculations proved to be sufficiently stable. This suggests that the force field used in the molecular dynamic simulations should be appropriate and capable of accurately analyzing the entry and diffusion process of these compounds.

3.2 Molecular Dynamics Simulations

As mentioned in the previous section, the permeation of pollutants through the membrane was simulated using CMD in combination with the umbrella sampling technique. The free energy profiles obtained via WHAM from simulations conducted separately for each of the studied PCBs are presented in Fig. 3.

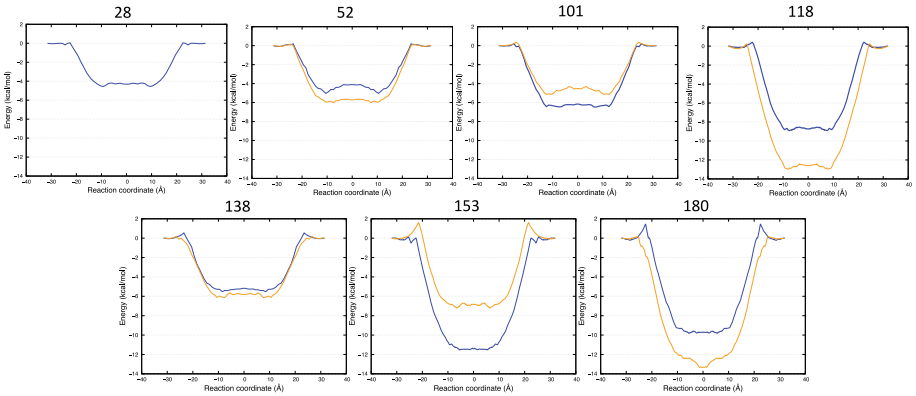

Fig. 3. Free energy diffusion profiles. Conformer with an angle smaller than 180° (blue line) and conformer with an angle greater than 180° (orange line).

The hydrophobic nature of the contaminants facilitates their penetration through the lipid bilayer, with a progressive decrease in free energy observed from the water-lipid interface to the hydrophobic region. Most of the conformers have their free energy minimum located about 7 Å from the center of the membrane, except for one conformer of PCB 180, which is situated near the center of the bilayer. In the other cases, a small increase in free energy is observed at the center of the membrane, resulting in slight local maxima. When comparing the conformers of different biphenyls, small shifts in the free energy minima are observed, indicating their preferred positions in the membrane. The most significant discrepancy is observed in the absolute values of the free energy minima, which in some cases reach up to 4 kcal/mol. This suggests that the entry may be slightly more favorable depending on the contaminant's conformation.

Destabilizations within the bilayer and shifts toward the more hydrophilic regions can be attributed to differences in the polar character of the conformers. Those exhibiting higher dipole moments tend to be less stable in the hydrophobic environment of the membrane. Furthermore, a direct correlation is observed between the free energy of the most stable conformation and the number of chlorine substitutions across the different biphenyls. However, PCB 118 deviates from this trend, displaying a lower free energy than more highly chlorinated compounds.

To demonstrate that the conformational barrier is energetically sufficient to ensure the existence of two conformers during entry into the lipid bilayer, Fig. 4 overlays the torsional potential energy profiles of biphenyls with 5, 6, and 7 substitutions, based on the torsional variation along the umbrella sampling simulation of each conformer. In all

cases, the stability of the conformer was confirmed throughout the trajectory, with no interchange between them at any point.

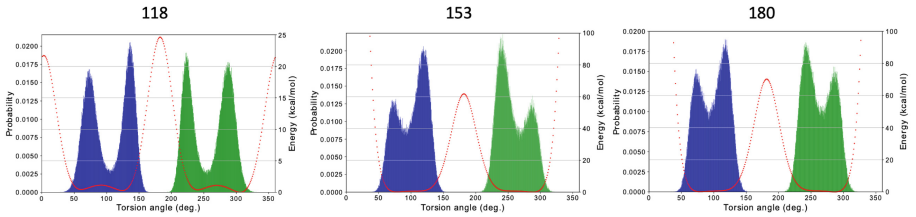

Fig. 4. Potential energy profiles (red dots) and dihedral angle count along the umbrella sampling. Conformer with an angle smaller than 180° (blue color) and conformer with an angle greater than 180° (green color).

3.3 Interaction Energy Decomposition Analysis

As explained above, a hybrid QM/MM method, which includes DFT for the QM region and electrostatic embedding for the QM/MM interaction, has been used to calculate the interaction energies. Specifically, the energetic analysis of intermolecular interactions between PCBs and the membrane was conducted in the regions of minimum free energy. The electrostatic, Pauli, induction, and dispersion contributions of the interaction energy were then obtained using the QM/MM-EDA scheme outlined in Methodology Section.

The first step in the QM/MM calculations is to determine the optimal size of the QM region. In this case, the QM region must include the pollutant and the minimum number of DOPC molecules required to ensure convergence of the total pollutant-lipid interaction energy and its individual components with respect to region size. Similar studies on other pollutants have determined this number using an arbitrary snapshot taken around the free energy minimum, ensuring that all energetic components converge within ± 1 kcal/mol when 10 residues are included in the QM region [23]. Once the number of lipids has been established, QM/MM-EDA calculations are performed at the free energy minima by sampling 34 geometries from the minima of the previous CMD simulations. In recent studies on the permeation of other systems through the same lipid membrane, the average values of the different interaction energy components were found to converge well after considering 100 geometries [17, 23]. However, more recent refinements have reduced this number to just over 30 geometries, balancing computational efficiency and accuracy in QM/MM calculations for systems with nearly a thousand atoms [24].

The preliminary mean values of total interaction energy and its components for PCB 118 and PCB 180 at the energy minima are summarized in Table 2. As observed, these values indicate that the previously reported anomaly in the energy profiles of PCB 118 disappears. A clear correlation is observed between the total interaction energy and the number of chlorine substituents. Dispersion energy emerges as the primary driving force behind intermolecular interactions within the lipid bilayer, consistent with the nonpolar nature and hydrophobic character of PCBs. An increase in chlorine substituents leads to higher dispersion energy, which, in turn, enhances the total interaction energy.

Table 2. Mean interaction energy and contribution values (kcal/mol) at the free energy minima for conformers with angles smaller and greater than 180°.

	E_{elec}	E_{Pau}	E_{disp}	E_{ind}	E_{int}
118 (<180°)	−16.49	46.10	−50.13	−6.77	−27.28
118 (>180°)	−17.34	49.45	−51.58	−6.99	−26.14
180 (<180°)	−19.57	55.06	−55.63	−7.35	−27.46
180 (>180°)	−18.32	51.28	−53.79	−6.87	−27.68

However, the energies obtained at the QM/MM level exhibit discrepancies compared to the classical free energy profile. In this case, conformer 2 of PCB 118 appears slightly more stable than conformer 1. Additionally, a significant increase in interaction energy is detected at the minima of both contaminants, suggesting that this difference may be attributed to entropic factors reflected in the free energy profiles.

In general, the small differences observed in the PCB entry processes, both in molecular dynamics simulations and QM/MM-EDA calculations, suggest that absorption and diffusion through the cell membrane are not the primary factors responsible for the differences in toxicity. Instead, the divergence appears to be linked to PCB metabolism.

In this context, affinity for the AhR receptor could explain the relative toxicity of these compounds. This receptor regulates the expression of genes associated with various disorders and diseases. When polychlorinated compounds enter the cell and bind to AhR, they induce changes in gene transcription, leading to toxic effects. Therefore, the affinity of PCBs for AhR may play a critical role in determining their toxicity and warrants further investigation in future studies. In the case of PCB 118, a PCB with dioxin-like toxicological properties, it exhibits a high affinity for AhR, while other SCB7 congeners show low or no affinity for the receptor.

4 Conclusions

In this work, a comparative study was conducted on the permeation of the contaminants that make up the SCB7 set through a lipid membrane formed by DOPC molecules, using a combination of classical molecular dynamics simulations, accelerated dynamics methods such as umbrella sampling, and a QM/MM-EDA approach. The molecular dynamics simulations demonstrated that the hydrophobic nature of PCBs favors their incorporation into the lipid bilayer, and that, in certain cases, differences between the conformers of PCBs are significant in terms of free energy. On the other hand, QM/MM-EDA calculations initially indicate that the number of chlorine substituents in the different biphenyls affects the interaction energy. In conclusion, the results suggest that absorption and diffusion steps through the cell membrane do not explain the toxicity differences measured for the SCB7 set, despite the small variations observed in the entry processes.

Acknowledgments. The authors thank the funding and support from the Diputación de Pontevedra and the University of Vigo. They also acknowledge the BioEDA project (PID2021-128180NB-I00) and GRC Xunta (ED431C 2024/21). N.R.B. thanks the University of Vigo for a postdoctoral

fellowship under the "Retención de Talento Investigador da Universidade de Vigo 2023" program. A.P.B. thanks the Xunta de Galicia for funding through the ED481A-2022/228 predoctoral fellowship.

Disclosure of Interests. The authors have no competing interests to declare that are relevant to the content of this article.

References

1. Ritter, L., Solomon, K.R., Forget, J., Stemeroff, M., O'Leary, C.: A review of selected persistent organic pollutants. In: International Programme on Chemical Safety (IPCS) PCS/95.39, p. 66. World Health Organization, Geneva (1995)
2. Wania, F., MacKay, D.: Tracking the distribution of persistent organic pollutants. Environ. Sci. Technol. **30**(9), 390A–396A (1996)
3. Van Den Berg, M., Birnbaum, L., Bosveld, A.T.C., Brunström, B., Cook, P., Feeley, M., Giesy, J.P., Hanberg, A., Hasegawa, R., Kennedy, S.W., Kubiak, T., Larsen, J.C., Van Leeuwen, F.X.R., Liem, A.K.D., Nolt, C., Peterson, R.E., Poellinger, L., Safe, S., Schrenk, D., Tillitt, D., Tysklind, M., Younes, M., Wærn, F., Zacharewski, T.: Toxic equivalency factors (TEFs) for PCBs, PCDDs, PCDFs for humans and wildlife. Environ. Health Perspect. **106**(12), 775–792 (1998)
4. Rappe, C.: Dioxin, patterns and source identification. Fresenius J. Anal. Chem. **348**(1–2), 63–75 (1994)
5. Beck, H., Droß, A., Eckart, K., Mathar, W., Wittkowski, R.: PCDDs, PCDFs and related compounds in paper products. Chemosphere. **19**(1–6), 655–660 (1989)
6. Merrill, M.L., Emond, C., Kimi, M.J., Antignaci, J.-P., Bizeci, B.L., Birnbaum, K.C.L.S., Barouki, R.: Toxicological function of adipose tissue: Focus on persistent organic pollutants. Environ. Health Perspect. **121**(2), 162–169 (2013)
7. Regnier, S.M., Sargis, R.M.: Adipocytes under assault: environmental disruption of adipose physiology. Biochim. Biophys. Acta Mol. basis Dis. **1842**(3), 520–533 (2014)
8. Nunes, T., González-Quijano-Mosteiro, A., Viñas, L.: Determinación de compuestos organoclorados en sedimentos de la Ría de Vigo. Procesos biogeoquímicos en sistemas costeros hispano-lusos. In: Prego, R., Fernández-Álvarez, J.M. (eds.) Diputación Provincial de Pontevedra, Vigo (1997)
9. González-Quijano, A., García, A., Fumega, J., González, J.: Temporal variation of PCB concentrations in mussel tissue in two areas of Santander Bay (Spain). Cienc. Mar. **32**(2B), 465–469 (2006)
10. Dickson, C.J., Madej, B.D., Skjevik, Å.A., Betz, R.M., Teigen, K., Gould, I.R., Walker, R.C.: Lipid14: the Amber lipid force field. J. Chem. Theory Comput. **10**(2), 865–879 (2014)
11. Wang, J., Wolf, R.M., Caldwell, J.W., Kollman, P.A., Case, D.A.: Development and testing of a general amber force field. J. Comput. Chem. **25**(9), 1157–1174 (2004)
12. Case, D.A., Belfon, K., Ben-Shalom, I.Y., Brozell, S.R., Cerutti, D.S., Cheatham III, T.E., Cruzeiro, V.W.D., Darden, T.A., Duke, R.E., Giambasu, G., et al.: AMBER 2020. University of California, San Francisco, CA (2020)
13. Kumar, S., Rosenberg, J.M., Bouzida, D., Swendsen, R.H., Kollman, P.A.: The weighted histogram analysis method for free-energy calculations on biomolecules. I. The method. J. Comput. Chem. **13**(8), 1011–1021 (1992)
14. Mandado, M., Hermida-Ramón, J.M.: Electron density based partitioning scheme of interaction energies. J. Chem. Theory Comput. **7**(3), 633–641 (2011)

15. Ramos-Berdullas, N., Pérez-Juste, I., Van Alsenoy, C., Mandado, M.: Theoretical study of the adsorption of aromatic units on carbon allotropes including explicit (empirical) DFT dispersion corrections and implicitly dispersion-corrected functionals: The pyridine case. Phys. Chem. Chem. Phys. **17**, 575–587 (2014)
16. Pérez-Barcia, A., Cárdenas, G., Nogueira, J.J., Mandado, M.: Effect of the QM size, basis set and polarisation on QM/MM energy decomposition analysis. J. Chem. Inf. Model. **63**(3), 882–897 (2023)
17. Alvarado, R., Cárdenas, G., Nogueira, J.J., Ramos-Berdullas, N., Mandado, M.: On the permeation of polychlorinated dibenzodioxins and dibenzofurans through lipid membranes: classical MD and hybrid QM/MM-EDA analysis. Membranes. **13**(28), 1–14 (2023)
18. Frisch, M.J., Trucks, G.W., Schlegel, H.B., Scuseria, G.E., Robb, M.A., Cheeseman, J.R., Scalmani, G., Barone, V., Petersson, G.A., Nakatsuji, H., et al.: Gaussian 16 Revision C.01. Gaussian, Inc., Wallingford, CT (2016)
19. Zhao, Y., Truhlar, D.G.: The M06 suite of density functionals for main group thermochemistry, thermochemical kinetics, non-covalent interactions, excited states, and transition elements: two new functionals and systematic testing of four M06-class functionals and 12 other functionals. Theor. Chem. Accounts. **120**, 215–241 (2008)
20. Cárdenas, G., Lucia-Tamudo, J., Mateo-delaFuente, H., Palmisano, V.F., Anguita-Ortiz, N., Ruano, L., Pérez-Barcia, A., Díaz- Tendero, S., Mandado, M., Nogueira, J.J.: MoBioTools: a toolkit to setup QM/MM calculations. J. Comput. Chem. **44**(4), 516–533 (2022)
21. Cárdenas, G. MoBioTools: https://github.com/mobiochem/MoBioTools, last accessed 20 March 2025
22. Mandado, M., Van Alsenoy, C. EDA-NCI: Energy Decomposition Analysis of Non-Covalent Interactions: https://github.com/marcos-mandado/EDA-NCI, last accessed 20 March 2025
23. Cárdenas, G., Pérez-Barcia, A., Mandado, M., Nogueira, J.J.: Characterization of cisplatin/membrane interactions by QM/MM energy decomposition analysis. Phys. Chem. Chem. Phys. **23**, 20533–20540 (2021)
24. Ruano, L., Pérez-Barcia, Á., Palmisano, V.F., Nogueira, J.J., Mandado, M., Ramos-Berdullas, N.: Unravelling the Role Played by Non-Covalent Interactions in the Action Mechanism of PCDDs within Cells, in preparation (2025)